APPLIED ORGANOMETALLIC CHEMISTRY
Appl. Organometal. Chem. **12**, 843–853 (1998)

Silicon-Modified Carbohydrate Surfactants IX: Dynamic Wetting of a Perfluorinated Solid Surface by Solutions of a Siloxane Surfactant Above and Below the Critical Micelle Concentration

R. Wagner,[1]* Y. Wu,[1] L. Richter,[1] S. Siegel,[1] J. Weissmüller[2] and J. Reiners[2]
[1]Max-Planck-Institute for Colloids and Surfaces, Rudower Chaussee 5, 12489 Berlin, Germany
[2]Bayer AG, 51368 Leverkusen, Germany

The dynamic wetting behaviour on a perfluorinated, low-energy solid has been investigated for a carbohydrate-modified phenylsiloxane surfactant. The surfactant concentration, the rate of interface generation and the [solid/liquid interface area] : [liquid/vapour interface area] ratio were varied systematically. Dynamic data for the liquid/vapour (γ_{lv}) and solid/liquid (γ_{sl}) interfacial tension as well as their Lifshitz–van der Waals and donor–acceptor contributions were determined under strictly controlled conditions. Since γ_{sl} reacts sensitively to variations of the surfactant concentration and the rate of interface generation, the covering of the liquid/nonpolar solid interface is assumed to be a spreading limiting factor. The corresponding γ_{lv} values remain constant and close to those obtained under equilibrium conditions. © **1998 John Wiley & Sons, Ltd.**

Keywords: carbohydrate-modified phenylsiloxane; surfactants; wetting behaviour; superspreading

Received 23 December 1997; accepted 2 June 1998

* Correspondence to: R. Wagner, Max-Planck-Institute for Colloids and Surfaces, Rudower Chaussee 5, 12489 Berlin, Germany.
Contract/grant sponsor: German Ministry for Research and Technology; Contract/grant number: 0310317 A/B.
Contract/grant sponsor: Deutsche Forschungsgemeinschaft; Contract/grant number: WA 1043/1-2.

1 INTRODUCTION

An exceptional property of aqueous solutions of certain trisiloxane surfactants is their ability to wet low-energy surfaces rapidly[1] (e.g. polyethylene, polypropylene, layers of natural waxes). Commercially available products (e.g. Silwet L77, Union Carbide) usually consist of complex mixtures bearing species with 4–12 ethylene oxide units attached to the trisiloxane moiety. So far, the active species within these mixtures have not been identified.

Chemical, geometrical, kinetic and energetic influences have been found to govern the superspreading process.[1–5] First, dynamic surface tension and dynamic interfacial tension measurements[6] have been carried out for the system of aqueous silicon-surfactant solution vs n-alkanes. Although liquid/liquid interfacial tension measurements cannot simulate the situation at the solid/liquid interface (e.g. the smoothness of an oil phase, partial surfactant solubility in it) the data suggest that bulk diffusion coefficients of superspreaders are one order of magnitude higher than those of conventional surfactants. Since hydrodynamics and a surfactant's adsorption kinetics have a complex influence on the dynamic contact angle,[7] a precise description of the fast-progressing wetting of a low-energy solid by a silicon-surfactant solution remains a challenging task.

In order to improve understanding of this process, solutions of strictly defined surfactants have to be investigated. Depending on the nature of a solid substrate, short-range polar forces and long-range forces of the Lifshitz–van der Waals type can emerge at interfaces. Their proportions have to be measured and, if possible, controlled. The obvious bulk-concentration effect has to be quantified for

 CCC 0268–2605/98/120843–11 $17.50

the liquid/vapour as well as the solid/liquid interface under dynamic conditions. Since dynamic wetting situations are essential for a broad spectrum of industrial applications, surfactants and solid surfaces of practical importance have to be considered for such investigations.

Therefore we initiated a comprehensive investigation of the wetting behaviour of strictly defined silicon surfactants. Silicon-modified carbohydrate surfactants of the siloxane, carbosilane, polysilane and silane types have been synthesized.[8–10]

In a further step we were able to quantify the impacts of substructures (silicon moiety, spacer, carbohydrate unit, modifying element) on the equilibrium wetting behaviour of dilute aqueous surfactant solutions on perfluorinated solid surfaces.[11,12] To ensure comparability with analogous data for liquid silicon precursors,[10,13] we focused our attention initially on surfactant solutions above the critical micelle formation concentration (cmc). It could be demonstrated that surface tension (γ_{lv}) and solid/liquid interfacial tension (γ_{sl}) develop independently. Determination of the Lifshitz–van der Waals (LW) and donor–acceptor (+/−) contributions proved the dominance of LW forces at the liquid–vapour interface. At the solid–liquid interface a structure-dependent balance between both contributions exists.

Recently[14] we investigated the effect of the surfactant concentration on the liquid/vapour and solid/liquid interfacial tensions and the corresponding interface covering. For all substances under investigation we found cmc(γ_{lv}) = cmc(γ_{sl}) and a dramatic increase in the donor–acceptor contributions below the cmc. From the slopes of the γ_{lv}–log c and γ_{sl}–log c isotherms we determined that the coatings of both the liquid-vapour and the solid-liquid interfaces were even. This finding differs remarkably from the proposed unsteady adsorption of sodium dodecylsulphate onto PTFE.[15]

Spreading is a dynamic process, however. Constant surfactant concentrations at the edge of fast-spreading drops cannot be assumed. If this is true, major shifts of the interfacial energies under dynamic conditions have to be expected. Therefore it is the purpose of this paper to examine the impacts of the surfactant concentration, the rate of interface generation and the [solid/liquid interface area] : [liquid/vapour interface area] ratio on the development of γ_{lv} and γ_{sl} under dynamic conditions.

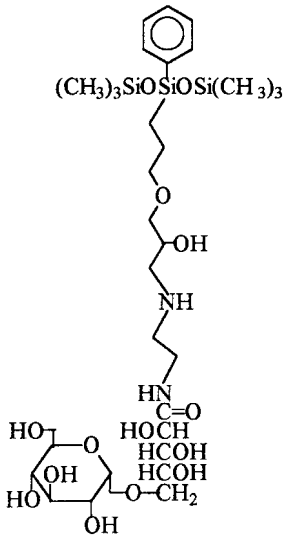

Figure 1 Structure of the carbohydrate-modified trisiloxane surfactant **1**.

2 MATERIALS AND METHODS

2.1 Materials

Since the single components of the superspreader mixtures have not been available, a strictly defined carbohydrate-modified trisiloxane surfactant **1** (Fig. 1) has been chosen to prove the practicability of our approach for the determination of dynamic wetting data. The synthesis and chemical characterization of this compound were described earlier.[10]

2.2 Methods

Distilled water has been used for the preparation of all surfactant solutions.

We used V2A steel and FEP® plates (tetrafluoroethylene–hexafluoropropylene copolymer; Du Pont) to determine the equilibrium and dynamic values for the liquid/vapour and solid/liquid interfacial energies. They were cleaned initially in ethanol, acetone and diethyl ether, and subsequently treated several times in an oxidizing solution consisting of conc. H_2SO_4, H_2O and $K_2S_2O_8$ (39:11:2 by wt) After these oxidations, water spreads on V2A steel plates and forms a contact angle of 116–117 ° on FEP®. Before every wetting experiment the plates were treated in this oxidizing solution for 30 min, carefully rinsed with bidistilled water and dried with argon.

The determination of the equilibrium contact angles of the aqueous surfactant solutions has been described in a companion paper[14] The liquid/vapour interfacial tension (γ_{lv}) (σ, ring method, data corrected according to Ref.[16]) and wetting tension α (Wilhelmy method) were measured independently (Young's equation)[17] (Eqn [1]).

$$\frac{\gamma_{sv} - \gamma_{sl}}{\gamma_{lv}} = \frac{\alpha}{\sigma} = \cos\theta \qquad [1]$$

To measure the equilibrium wetting tension α, an FEP® plate of defined width and thickness was dipped stepwise (2 mm per step, usually 10–15 steps) into a surfactant solution of known concentration. The force (p) measured correlates with α (Eqn [2]).

$$P = u\alpha - \rho g d b x_i \qquad [2]$$

where

u = perimeter of plate
ρ = liquid density
g = gravitational constant
m = mass of liquid in meniscus
d = thickness of plate
b = width of plate
x_i = immersion depth of plate

We measured the force after 5 min. This time was found to be necessary for the system to reach a force equilibrium between the advance of the meniscus induced by wetting tension and the meniscus weight. In this equilibrium state the meniscus of the surfactant solution does not advance or recede any further and the measured force remains constant. Plotting the force values p against the immersion depth x_i yields, after extrapolation to $x_l = 0$, the product of wetting tension α and perimeter u (Eqn [2]).

This general procedure was repeated for diluted surfactant solutions in the range from 10^{-2} to 10^{-7} mol dm^{-3}.[14] All measurements were carried out at 20 °C.

The interfacial tension γ_{sl} could be calculated from the γ_{sv}–α relationship (see Eqn [1]).

The procedure for the determination of the solid/vapour interfacial tension (γ_{sv}) of the non-polar FEP® ($\gamma_{sv} = \gamma_{sv}^{LW} = 18.9$ mN m^{-1}) was described earlier.[11]

We also determined the Lifshitz–van der Waals contributions to the liquid/vapour[18] (γ_{lv}^{LW} (Eqn [3]) and solid/liquid[19] (γ_{sl}^{LW}) (Eqn [4]) interfacial tensions.

$$\gamma_{lv}^{LW} = \left[\frac{\gamma_{lv}(1+\cos^{\theta})}{2\sqrt{\gamma_{sv}^{LW}}}\right]^2 \qquad [3]$$

$$\gamma_{sl}^{LW} = \gamma_{sv}^{LW} + \gamma_{lv}^{LW} - 2\sqrt{\gamma_{sv}^{LW}\gamma_{lv}^{LW}} \qquad [4]$$

The donor–acceptor portions ($\gamma_{lv}^{+/-}$) and ($\gamma_{sl}^{+/-}$) were calculated according to Fowkes' approach[20] (Eqns [5] and [6].

$$\gamma_{lv} = \gamma_{lv}^{LW} + \gamma_{lv}^{+/-} \qquad [5]$$

$$\gamma_{sl} = \gamma_{sl}^{LW} + \gamma_{sl}^{+/-} \qquad [6]$$

The characterization of the dynamic wetting behaviour of a rapidly spreading drop, either by direct observation of the angle at the progressing three-phase contact line or by dynamic measurements of the liquid/vapour and solid/liquid interfacial tensions under controlled and reproducible conditions, is as yet an unsolved problem.

It is our basic assumption that key aspects of such a spreading process can be simulated by immersion of a well-defined solid into a surfactant solution. A movement of surfactant molecules from the bulk via the liquid/vapour interface to the solid/liquid interface should be influenced by a number of factors (Fig. 2). The rate of solid/liquid interface generation (rig, which depends on the immersion speed and the plate geometry) and surfactant's bulk concentration (c) should play major roles. Further,

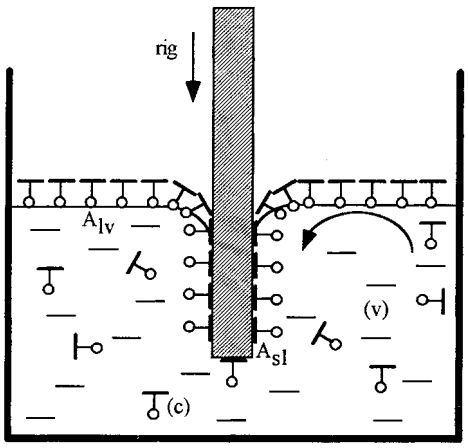

Figure 2 Parameters influencing the dynamic wetting of a low-energy material.

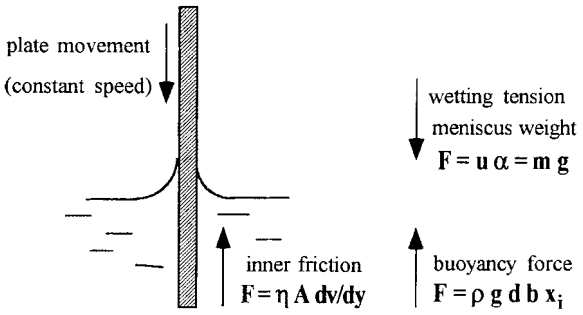

Figure 3 Force balance at plates under dynamic conditions.

the immersion-depth-dependent absolute area of the solid/liquid interface (A_{sl}), its ratio with the constant liquid/vapour interface area (A_{lv}) and the solution volume (v) have also to be considered.

We used a Wilhelmy-method based algorithm which by-passes the troublesome simultaneous determination of both interfacial energies. One completely wettable V2A steel plate and one FEP® plate of identical geometry were immersed in separate runs in a given surfactant solution.[21] Despite identical pretreatments, exploratory experiments with other than our 'standard plates' yielded slightly shifted force values. Therefore this strategy should not be considered to accelerate the data acquisition.

The parallel experiments were carried out under strictly identical conditions (immersion speed, vessel geometry, surfactant solution volume, liquid/vapour interface area surface ageing after sucking the solution off [30 min]). The force in both runs was measured at the same immersion depths

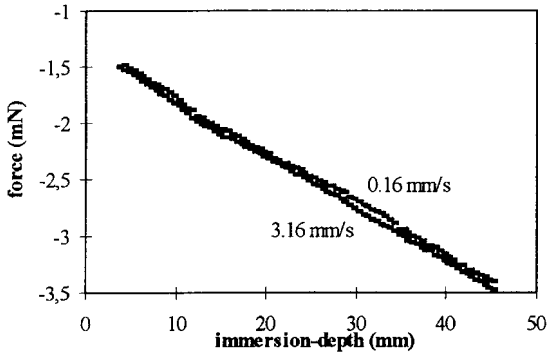

Figure 4 Friction effect of the immersion speed on the force (p) versus immersion-depth (x_i): curve for water on FEP® (plate geometry: width 18.2 mm, thickness 0.245 mm)

(i.e. from the contact with the liquid surface in 0.5 mm steps). The force data from the V2A steel plate experiment provided information on the dynamic surface tension of the solution whereas the FEP® plate data characterized the dynamic wetting tension. Extensive exploratory experiments showed that under dynamic conditions the influence of friction between the solid surface and the liquid on the force balance could not be excluded[7] (Figs 3 and 4). Typically we found a friction term in the range of 3–5 mN m^{-1} for immersion velocities >0.8 mm s^{-1}.

For surfactant solutions under dynamic conditions (Fig. 3) the forces at the V2A steel plate (p_s^{σ}, determination of the liquid/vapour interfacial tension) and the FEP® plate (p_s^{α}, wetting tension determination) can be expressed by Eqns [7] and [8]

$$P_s^{\sigma} = u\sigma_s - \rho g d b x_i - \eta A \frac{dv}{dy} \quad [7]$$

$$P_s^{\alpha} = u\alpha_s - \rho g d b x_i - \eta A \frac{dv}{dy} \quad [8]$$

where

σ_σ = dynamic liquid/vapour interfacial tension
α_s = dynamic wetting tension
η = liquid viscosity
A = immersed plate area
dv/dy = derivate of the liquid velocity with respect to the distance to the solid plate surface

We failed to eliminate mathematically the immersion-speed-dependent friction effect, in analogy to the immersion-depth-related buoyancy effect (Eqn [2]), but if the approximation $\eta_{\text{surfactant solution}} \approx \eta_{\text{water}}$ holds sufficiently well one can eliminate the friction term by immersion experiments with pure water carried out under conditions identical to those for surfactant solutions. The liquid/vapour interfacial tension (σ_w) of pure water at 20 °C is well known (72.6 mN m^{-1}) and its wetting tension (α_w) on FEP® (-29.4 mN m^{-1}) can be determined separately under equilibrium conditions. The identity between equilibrium and dynamic interfacial energies for pure liquids is well established.[7,22]

For pure water under dynamic conditions the forces at the V2A steel plate (p_w^{σ}, determination of the liquid/vapour interfacial tension) and the FEP® plate (p_w^{α}, wetting tension determination) can be expressed by Eqns [9] and [10].

Table 1 Concentration dependence of the interfacial properties at equilibrium for the phenyl-substituted trisiloxane derivative

Concn (mol dm^{-3})	γ_{lv} (mN m^{-1})	γ_{lv}^{LW} (mN m^{-1})	$\gamma_{lv}^{+/-}$ (mN m^{-1})	γ_{sl} (mN m^{-1})	γ_{sl}^{LW} (mN m^{-1})	$\gamma_{sl}^{+/-}$ (mN m^{-1})	α (mN m^{-1})	$\cos\theta$	θ (deg)
3.0×10^{-3}	24.9	21.5	3.4	3.5	0.08	3.42	15.4	0.618	52
1.0×10^{-3}	24.4	21.5	2.9	3.0	0.08	2.92	15.9	0.683	47
7.5×10^{-4}	24.4	22.3	2.1	2.2	0.14	2.06	16.7	0.651	49
5.8×10^{-4}	25.3	22.6	2.7	2.8	0.17	2.63	16.1	0.635	51
4.2×10^{-4}	25.7	22.4	3.3	3.4	0.15	3.25	15.5	0.603	53
2.1×10^{-4}	26.2	19.1	7.1	7.1	0.00	7.10	11.8	0.451	63
1.1×10^{-4}	29.3	20.3	9.0	9.0	0.03	8.97	9.9	0.340	70
7.5×10^{-5}	29.5	20.4	9.1	9.1	0.03	9.07	9.8	0.332	71
4.7×10^{-5}	36.2	17.9	18.3	18.3	0.01	18.25	0.6	0.016	89
2.7×10^{-5}	42.9	16.6	26.3	26.4	0.07	26.33	−7.5	−0.174	100
1.5×10^{-5}	48.7	17.7	31.0	31.0	0.02	30.98	−12.1	−0.249	104
8.2×10^{-6}	57.4	23.6	33.8	34.0	0.26	33.74	−15.1	−0.264	105
4.9×10^{-6}	65.9	19.1	46.8	46.8	0.00	46.80	−27.9	−0.423	115
2.0×10^{-6}	70.4	23.2	47.2	47.4	0.22	47.18	−28.5	−0.405	114
5.3×10^{-7}	72.7	23.8	48.9	49.2	0.28	48.92	−30.3	−0.416	115

$$P_w^{\sigma} = u\sigma_w - \rho g d b x_i - \eta A \frac{dv}{dy} \quad [9]$$

$$P_w^{\alpha} = u\sigma_w - \rho g d b x_i - \eta A \frac{dv}{dy} \quad [10]$$

Subtraction of Eqn [9] from Eqn [7] and Eqn [10] from Eqn [8] yields Eqns [11] and [12].

$$p_s^{\sigma} - p_w^{\sigma} = u\sigma_s - u\sigma_w \quad [11]$$

$$p_s^{\alpha} - p_w^{\alpha} = u\alpha_s - u\alpha_w \quad [12]$$

and finally Eqns [13] and [14];

$$\frac{p_s^{\sigma} - p_w^{\sigma} + u\sigma_w}{u} = \sigma_s \quad [13]$$

$$\frac{p_s^{\alpha} - p_w^{\alpha} + u\alpha_w}{u} = \alpha_s \quad [14]$$

A computer-controlled combination of the force values obtained for surfactant solutions and pure water at identical immersion depths (Eqns [13] and [14]) makes accessible dynamic data for the liquid/vapour interfacial tension and the wetting tension. They can be used to describe the dynamic development of contact angles (Eqn [1]), Lifshitz–van der Waals contributions of the liquid/vapour (Eqn [3]) and solid/liquid (Eqn [4]) interfacial tensions as well as the complementary donor–acceptor contributions (Eqns [5] and [6]).

The authors are well aware that this type of dynamic data does not reflect intrinsic solution properties. The system is forced to respond to defined changes of certain parameters. Therefore trends and mechanisms, rather than intrinsic kinetic constants, are disclosed.

3 RESULTS

In Table 1 and Fig. 5 the concentration-dependent data under equilibrium conditions for the interfacial energies, their Lifshitz–van der Waals and donor–acceptor contributions, as well as the contact angles, are summarized. Characteristic aspects are the practical convergence of cmc(γ_{lv}) and cmc(γ_{sl}),

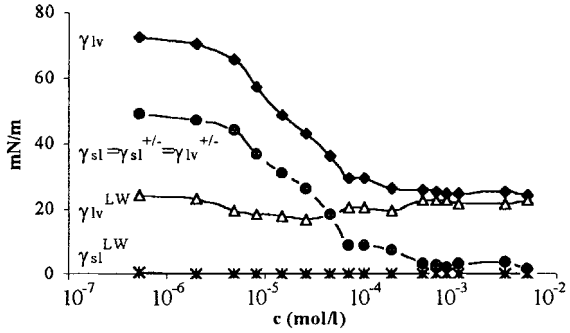

Figure 5 Equilibrium values of the liquid/vapour and solid/liquid interfacial tensions on FEP®; donor–acceptor (+/−) and Lifshitz–van der Waals (LW) contributions are shown for **1** at concentration *c*

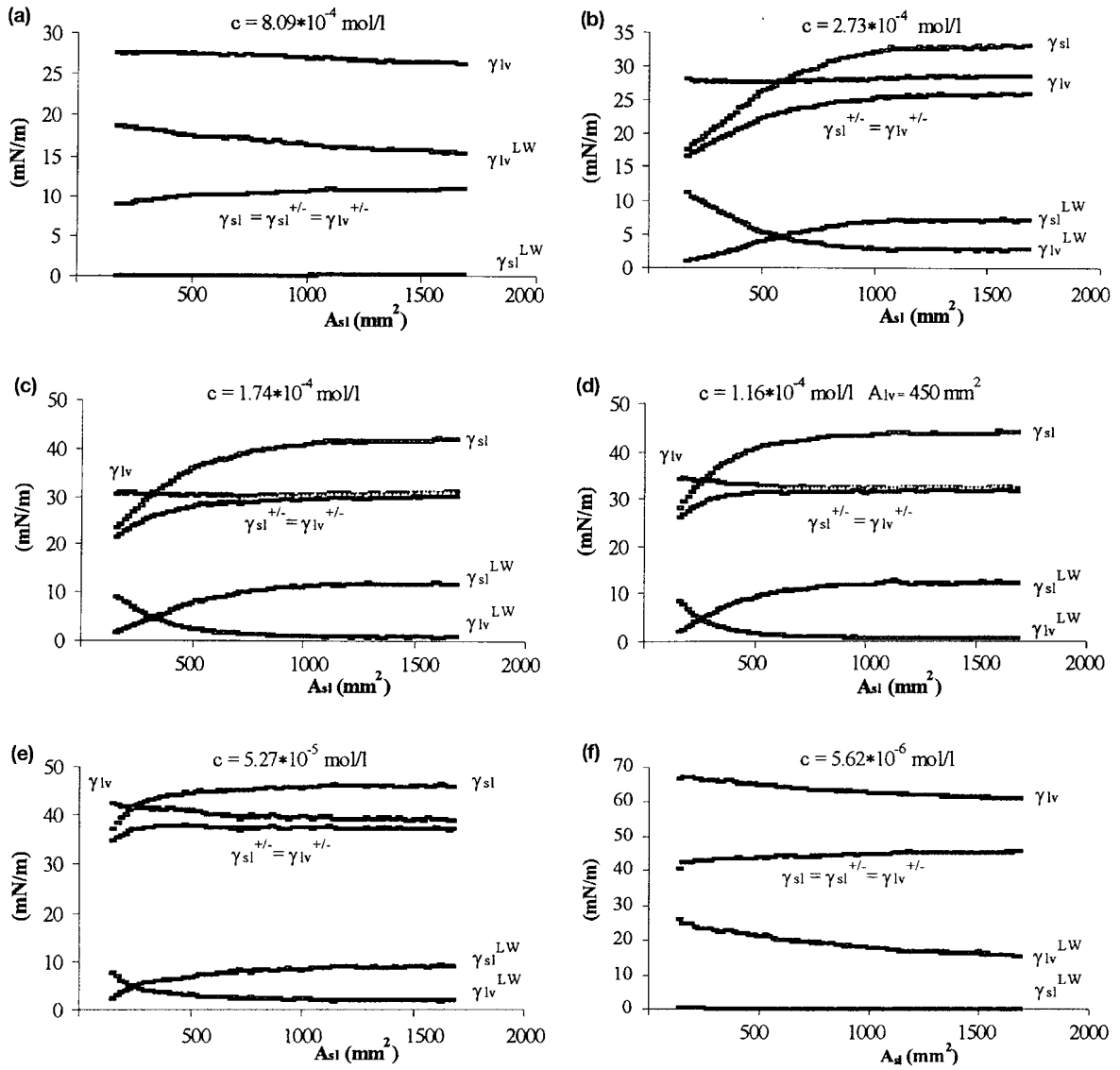

Figure 6 Concentration-dependent dynamic liquid/vapour (γ_{lv}) and solid/liquid (γ_{sl}) interfacial tensions and their Lifshitz–van der Waals and donor–acceptor contributions (parameters: rate of solid/liquid interface generation, rig = 116 mm^2 s^{-1} [V2A and FEP® plates, width 18.2 mm, thickness 0.245 mm, immersion speed 3.16 mm s^{-1}], volume of surfactant solution 100 ml, area of the liquid/vapour interface, A_{lv} = 450 mm^2). The concentration c of surfactant **1** is shown on each graph.

the polar nature of γ_{sl} ($\approx \gamma_{sl}^{+/-}$) and the minimum of γ_{lv}^{LW} below the cmc.

Figure 6 describes the concentration dependence of γ_{lv} and γ_{sl} under high-rate dynamic wetting conditions. For concentrations at and below the cmc (Fig. 6b–e) γ_{sl} reacts sensitively to an increase of the solid/liquid interface area (A_{sl}). A significant Lifshitz–van der Waals contribution (γ_{sl}^{LW}) emerges. Above the cmc (Fig. 6a) and in extremely dilute solutions close to water (Fig. 6f) an equilibrium-like force pattern ($\gamma_{sl} \approx \gamma_{sl}^{+/-} = \gamma_{lv}^{+/-}$; $\gamma_{sl}^{LW} \approx 0$) is found.

Figure 7 characterizes a low rate dynamic wetting situation. Over the whole concentration range, γ_{lv} and γ_{sl} remain close to equilibrium. A slip–stick effect has already been described

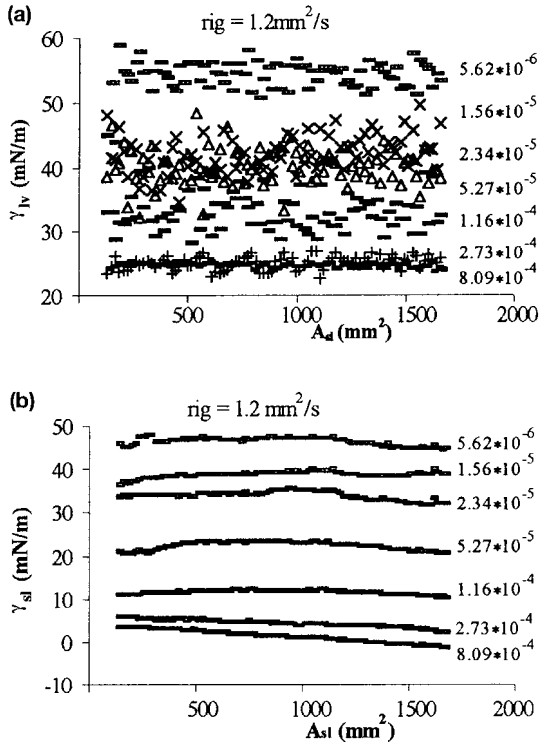

Figure 7 Concentration dependence of (a) γ_{lv} and (b) γ_{sl} (rig = 1.2 mm^2 s^{-1}, immersion speed 0.033 mm s^{-1}; for other parameters see Fig. 6).

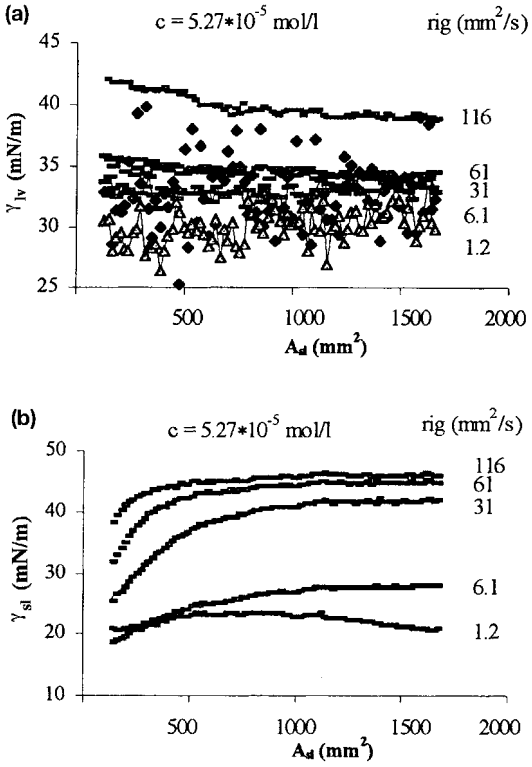

Figure 8 Influence of the rate of solid/liquid interface generation rate (rig) on (a) γ_{lv} and (b) γ_{sl} ($c = 5.27 \times 10^{-5}$ mol l^{-1}; for other parameters see Fig. 6).

for slow dynamic wetting experiments.[26] We attribute the slip–stick effect of some γ_{lv} curves to the inevitable micro-roughness of the steel plate.

Figure 8 describes the divergent responses of γ_{lv} and γ_{sl} on a systematic variation of the rate of solid/liquid interface generation rate (rig). For γ_{lv} a minor increase of a few mN/m is found. However, γ_{sl} reacts with a steep increase to an acceleration of the wetting process. The slip–stick effect disappears at higher rates of solid/liquid interface generation.

Figure 9 concerns the influence of the liquid/vapour interface area (A_{lv}) on the wetting behaviour under high-rate conditions. Above the cmc (Fig.9a) and in diluted systems (Fig. 9b) no significant dependence was found.

Figure 10 (see also Fig. 6d) indicates that for medium concentrations under high-rate conditions two wetting states exist. An equilibrium-like force pattern is found for large liquid/vapour interfaces (Fig. 10b). A reduction in the liquid/vapour interface creates a situation where γ_{sl} exceeds γ_{lv} and a considerable γ_{sl}^{W} contribution appears.

4 DISCUSSION

4.1 Concentration dependence

In contrast to the extensively investigated wetting behaviour of pure liquids on solid surfaces,[23,24] few systematic data are accessible in the literature concerning surfactant concentration dependence and/or the dynamic behaviour of the solid/liquid interfacial tension. Whereas for pure liquids under moderate dynamic conditions, constant γ_{lv}, γ_{sl} and contact angle values are found,[22,25,26] for completely miscible two-component systems a steady behaviour cannot be expected.[27,28]

Despite the known concentration impact on the superspreading effect,[13] a detailed investigation of the dynamic situation at both the solid/liquid and liquid/vapour interfaces has not been carried out for silicon surfactants.

The characteristic aspects of the equilibrium behaviour at both interfaces (see Fig. 5) have been outlined in a companion paper:[14]

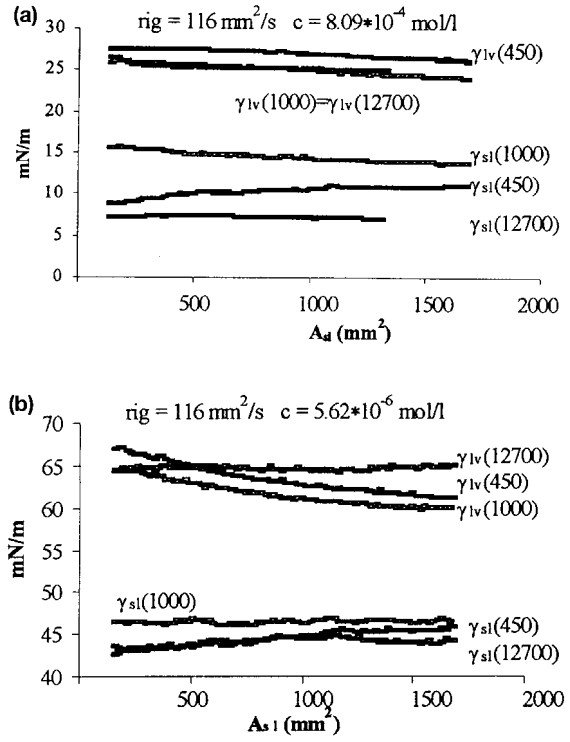

Figure 9 Influence of the ratio A_{sl}: A_{lv} on γ_{lv} and γ_{sl}. Three different vessels with liquid/vapour interface areas (A_{lv}) of 12700 mm^2, 1000 mm^2 and 450 mm^2 were used; maximum solid/liquid interface area (A_{sl}) at 45 mm immersion depth = 1660 mm^2, rig = 116 mm^2 s^{-1}, immersion speed 3.16 mm s^{-1}; for other parameters see Fig. 6.

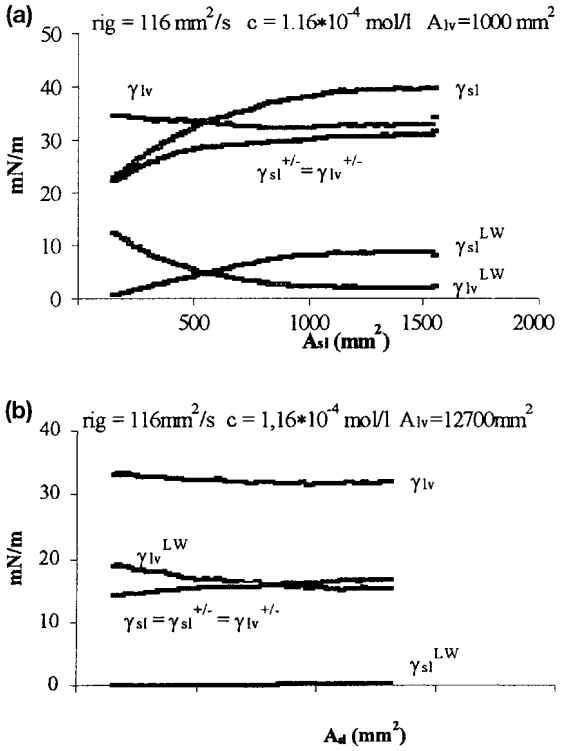

Figure 10 Medium surfactant concentrations: influence of the ratio A_{lv}: A_{sl} on γ_{lv} and γ_{sl} as well as their Lifshitz–van der Waals and donor–acceptor contributions (area of the liquid/vapour interface (A_{lv}) (a) 1000 mm^2 and (b) 12700 mm^2; for other parameters see Fig. 6).

(a) a cmc (γ_{sl}) exists close to the well-known cmc (γ_{lv});[29,30]
(b) above the cmc γ_{lv} is determined by the Lifshitz–van der Waals contribution whereas for γ_{sl} a structure-dependent balance between Lifshitz–van der Waals and donor–acceptor contributions exists;
(c) below the cmc the $\gamma_{lv}^{+/-}$ and $\gamma_{sl}^{+/-}$ contributions increase steeply with decreasing surfactant concentration and γ_{lv}^{LW} shows a significant minimum just within the concentration range characterized by the steepest γ_{lv} increase;
(d) diverging from the results for charged surfactants and/or surfaces,[15,31–33] for the non-polar fluorinated surface/non-ionic silicon surfactant system a concentration-dependent even adsorption at both interfaces takes place.

An ideal simulation of a spreading drop should fulfil the following conditions:

(1) the liquid volume remains constant;
(2) the areas of the solid/liquid (A_{sl}) and liquid/vapour (A_{lv}) interfaces increase rapidly relative to the drop volume:
(3) the ratio $A_{sl} : A_{lv}$ increases.

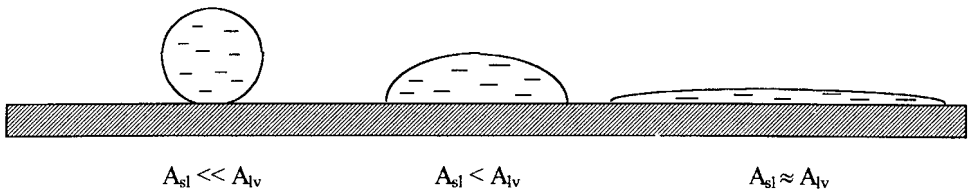

Figure 11 Evolution of the solid/liquid (A_{sl}) and liquid/vapour (A_{lv}) interfaces of a spreading drop.

We are aware that in this sense a surface increase by immersion of a plate is not strictly equivalent to a fast-spreading drop. In our experiments A_{lv} is constant. Thus, despite a possibly high increase in absolute A_{sl}, we cannot simulate the rapidly increasing $[A_{sl} + A_{lv}]$: [liquid volume] ratio-appearing in a spreading drop with a volume of a few microlitres.

Figure 6 illustrates the consequences of concentration variations to the interfacial energies under high solid/liquid interface generation conditions. Above the cmc (Fig. 6a) γ_{lv} and γ_{sl} are practically constant and γ_{lv} remains close to the equilibrium value (Fig. 5). But due to an increased $\gamma_{sl}^{+/-}$ contribution, γ_{sl} increases significantly. Nevertheless the interfacial balance is still determined by the properties of the surfactant molecules.

At and below the cmc (Fig. 6b–e) the situation changes dramatically and offers unexpected aspects. Despite the high immersion velocity, γ_{lv} was found to be constant and relatively close to equilibrium. Although somewhat surprised, we report its composition. A sharply declining Lifshitz–van der Waals contribution is compensated by an increasing donor–acceptor one. In fast dynamic modes the surface tension appears to be of an extremely polar nature. The authors assume an interrelation with the minimum of γ_{lv}^{LW} for medium concentrations in equilibrium[14] (see also Fig. 5). The lower the concentration, the more steeply γ_{sl} increases to a non-equilibrium value and simultaneously exceeds γ_{lv}. Intriguingly, $\gamma_{sl}^{+/-}$ and $_{sl}^{LW}$ contribute to this increase. The often-observed[11–14] equilibrium pattern $\gamma_{sl} \approx \gamma_{sl}^{+/-} = \gamma_{lv}^{+/-}$ is not valid here. In contrast to γ_{lv}, which is determined by the donor–acceptor force (and which is not well understood) a Lifshitz–van der Waals-force-influenced γ_{sl} emerges.

At very low surfactant concentrations (Fig. 6f) the system returns to a force pattern relatively close to that of the equilibrium state, where water properties dominate the interfacial balances.

4.2 Rate of solid/liquid interface generation

The results presented above immediately raise the question of the role of the solid/liquid interface generation rate. Figure 7 proves that a very low rate ($1.2\ mm^2\ s^{-1}$) gives the system the chance to maintain an equilibrium wetting state over the whole concentration range.

The influence of the solid/liquid interface generation rate was investigated in detail for medium concentrations (Fig. 8). It becomes clear that the change from an equilibrium-like regime ($1.2\ mm^2\ s^{-1}$) to a typical dynamic one proceeds at the relatively low rate of $6.1\ mm^2\ s^{-1}$. The higher the rate, the more pronounced the difference from the equilibrium state. Whereas the immersion-rate-dependent increase of γ_{lv} amounts to a few mN/m $_{sl}$ is shifted to values close to that of pure water.

4.3 Ratio of the areas of the solid/liquid (A_{sl}) and liquid/vapour (A_{lv}) interfaces

We stated earlier that in a real spreading process the A_{sl}:A_{lv} ratio increases with time. For an extended, almost flat, drop in a late stage of evolution, rough identity of both interfacial areas can be assumed (Fig. 11). The dynamic wetting experiments described so far have been carried out in a 100 ml vessel with a constant A_{lv} of $450\ mm^2$. During the immersion of the plates (depth 45 mm) A_{sl} increased from zero to about $1660\ mm^2$. Thus, it even exceeded the corresponding liquid/vapour interfacial area A_{lv}. It becomes clear that a systematic variation of A_{lv} can be used in order to characterize the (energetically) different stages of drop evolution.

Above the cmc (Fig. 9a) the pattern already discussed (with constant γ_{lv} close to equilibrium and a constant but increased γ_{sl}) was found. We did not find any notable influence of the ratio of the interfacial areas on the energy balance.

The same is true for diluted systems close to the composition of pure water (Fig. 9b). Both interfacial energies remained constant and close to their equilibrium values.

Again the solutions of medium concentration showed intriguing behaviour (Figs. 6d, and 10). Whereas γ_{lv} remained close to equilibrium the development of γ_{sl} depended decisively on the A_{sl}:A_{lv} ratio. For high ratios (simulating a late stage of drop evolution; Figs. 6a, 10c and 11) we have already discussed the steeply increasing γ_{sl} and its remarkable composition ($\gamma_{sl}^{+/-}$ accompanied by a considerable γ_{sl}^{LW} contribution). For an extremely low ratio (characteristic for a very early stage of drop evolution; (Figs. 10b and 1) a force pattern similar to that of solutions above the cmc (Fig. 6a; $_{sl} < \gamma_{lv}$ and $\gamma_{sl} \approx \gamma_{sl}^{+/-}$) is found. Clearly high bulk concentrations and/or a considerable surfactant predeposition at the liquid/vapour interface enhance the more difficult covering of the solid/liquid interface.

The question arises of whether a consistent

description of the dynamic process can be developed from these single findings. The evaluation of the concentration-dependent surfactant solution behaviour under dynamic conditions allows to us draw a first conclusion. In the non-ionic siloxane surfactant solution–non-polar solid system the liquid/vapour interfacial tension (the adsorption of surfactant molecules to the liquid/vapour interface) appears to be no spreading-speed limiting factor. It reacts robustly in dynamic conditions. The sensitive response of the solid/liquid interfacial tension to concentration and the solid/liquid interface generation rate variations gives a hint as to what could limit the spreading process. Clearly, the formation of a sufficiently dense surfactant layer at the solid/liquid interface is a slow process. Since the variation of A_{lv} (adjusting the number of predeposited surfactant molecules) has a selective influence on the dynamic behaviour of γ_{sl}, the shift of molecules along the liquid/vapour interface is a necessary step but probably not a rate-determining one.

The data presented above show that the method is suitable to characterize quantitatively the dynamic behaviour of surfactant solutions. Depending on the surfactant concentration, three different dynamic wetting states exist. For solutions above and far below the cmc the equilibrium pattern $\gamma_{sl} \approx {\gamma_{sl}}^{+/-} = {\gamma_{lv}}^{+/-}$ and ${\gamma_{sl}}^{LW} \approx 0$ holds. Due to the appearance of a considerable ${\gamma_{sl}}^{LW}$ contribution γ_{sl} exceeds γ_{lv} at and slightly below the cmc. The sensitive response of γ_{sl} to changes of the surfactant concentration and the interface generation rate indicates that the adsorption onto the solid/liquid interface could be the limiting step during the wetting of low-energy substrates.

Nevertheless, a number of questions still remain. So far, commercially available superspreaders (i.e. the fast-spreading Silwet L77), or their single components, have not been tested. The carbohydrate-modified phenylsiloxane surfactant under investigation is regarded as a 'slow' surfactant. Since the dynamic development of γ_{sl} seems to be the limiting factor, the role of the intensively studied (intrinsic) dynamic (γ_{lv}) of superspreaders[34] has to be examined. Does a correlation exist between the two dynamic interfacial energies? Finally, it is of immediate practical importance to investigate other than perfluorinated solid surfaces.

Acknowledgment The 'Siloxanyl-modified carbohydrates' research project was supported financially by the German Ministry for Research and Technology (Reg. No. 0310317 A/B). The 'Polyhydroxylated silicon compounds' project is supported by the Deutsche Forschungsgemeinschaft (Reg. No. WA 1043/1-2).

REFERENCES

1. T. Stoebe, Z. Lin, R. M. Hill, M. D. Ward and H. T. Davis, *Langmuir* **12**, 337 (1996).
2. K. P. Ananthapadmanabhan, E. D. Goddard and P. Chandar, *Coll. Surf.* **44**, 281 (1990).
3. S. Zhu, W. G. Miller, L. E. Scriven and H. T. Davis, *Coll. Surf.* **90**, 63 (1994).
4. F. Tiberg and A. M. Cazabat, *Europhys. Lett.* **25**, 205 (1994).
5. F. Tiberg and A. M. Cazabat, *Langmuir* **10**, 2301 (1994).
6. T. Svitova, H. Hoffmann and R. M. Hill, *Langmuir* **12**, 1712 (1996).
7. G. Kretzschmar, *J. Inf. Rec. Mater.* **20**, 439 (1993).
8. R. Wagner, L. Richter, R. Wersig, G. Schmaucks, B. Weiland, J. Weissmüller and J. Reiners, *Appl. Organometal. Chem.* **10**, 421 (1996).
9. R. Wagner, L. Richter, B. Weiland, J. Weißmüller and J. Reiners, *Appl. Organometal. Chem.* **10**, 437 (1996).
10. R. Wagner, L. Richter, Y. Wu, B. Weiland, J. Weissmüller, J. Reiners, E. Hengge and A. Kleewein, *Appl. Organometal. Chem.* **12**, 47 (1998).
11. R. Wagner, L. Richter, J. Weissmüller, J. Reiners, K. -D. Klein, D. Schaefer and S. Stadtmüller, *Appl. Organometal. Chem.* **11**, 617 (1997).
12. R. Wagner, L. Richter, Y. Wu, J. Weissmüller, J. Reiners, E. Hengge and A. Kleewein, *Appl. Organometal. Chem.* **12**, 265 (1998).
13. R. Wagner, L. Richter, Y. Wu, J. Weissmüller, J. Reiners, E. Hengge, A. Kleewein and K. Hassler, *Appl. Organometal. Chem.* **11**, 645 (1997).
14. R. Wagner, L. Richter, Y. Wu, J. Weissmüller, J. Reiners and A. de Montigny, *Appl. Organometal. Chem.*, in press.
15. R. Knapikowski, U. Messow, K. Quitzsch and H. -G. Hauthal, *Chem. Technik* **44**, 339 (1992).
16. W. D. Harkins and H. F. Jordan, *J. Am. Chem. Soc.* **52**, 1751 (1930).
17. T. Young, *Phil. Trans. R. Soc.*, **95**, 65 (1805).
18. G. Czichocki, B. Gilsenbach, M. Olschewski and L. Richter, *Plaste Kautsch.* **34**, 445 (1987).
19. D. K. Owens and R. C. Wendt, *J. Appl. Polym. Sci.* **13**, 1741 (1969).
20. F. M. Fowkes, *Ind. Eng. Chem.* **56**, 40 (1964).
21. J. Guastalla, *J. Chim. Phys.* **51**, 583 (1954).
22. D. Y. Kwok, C. J. Budziak and A. W. Neumann, *J. Coll. Interface Sci.* **173**, 143 (1995).
23. M. E. Schrader and G. Leob, *Modern Approaches to Wettability*, Plenum Press, New York, 1991, Chapter 1, pp. 1–27.
24. M. E. Schrader and G. Leob, *Modern Approaches to Wettability*, Plenum Press, New York, 1991, Chapter 5, pp. 101–142.

25. R. V. Sedev, C. J. Budziak, J. G. Petrov and A. W. Neumann, *J. Coll. Interface Sci.* **159**, 392 (1993).
26. D. Y. Kwok, R. Lin, M. Mui and A. W. Neumann, *Coll. Surf. A* **116**, 63 (1996).
27. R. Knapikowski, U. Messow and K. Quitzsch, *Chem. Technik* **46**, 234 (1994).
28. R. J. Good and R. R. Stromberg, *Surface and Colloid Science*, Vol. 11, *Experimental Methods*, Plenum Press, New York, 1979, p. 22.
29. E. Wolfram and E. Boross-Vargha, *Ann. Univ. Sci. Budapest. Rolando Eötvös Nomin., Sect. Chim.* 37 (1969).
30. H. Haidara, M. K. Chaudhury and M. J. Owen, *J. Phys. Chem.* **99**, 8681 (1995).
31. V. V. Yaminski and K. B. Yaminskaya, *Langmuir*, **11**, 936 (1995).
32. K. Lunkenheimer and A. Heilig, *Z. Phys. Chem.* **263**, 593 (1982).
33. R. Miller, S. Treppo, A. Voigt, W. Zingg and A. W. Neumann, *Coll. Surf.* **69**, 203 (1993).
34. D. S. Murphy, G. A. Policello, E. D. Goddard and P. J. G. Stevens, Physical properties of silicone surfactants for agrochemical applications. In *Pesticide Formulations and Application Systems*, Vol. 12, Devisetty, B. N., Chasin, D. G. and Berger, P. D. (eds), ASTM STP 1146, Philadelphia, 1993, pp. 45–56.

